# Connecting -fluidics to electron microscopy

Kemmerling, Simon ; Ziegler, Jörg ; Schweighauser, Gabriel ; Arnold, Stefan A ; Giss, Dominic ; Müller, Shirley A ; Ringler, Philippe ; Goldie, Kenneth N ; Goedecke, Nils ; Hierlemann, Andreas ; Stahlberg, Henning ; Engel, Andreas ; Braun, Thomas

Abstract: A versatile methodology for electron microscopy (EM) grid preparation enabling total content sample analysis is presented. A microfluidic-dialysis conditioning module to desalt or mix samples with negative stain solution is used, combined with a robotic writing table to micro-pattern the EM grids. The method allows heterogeneous samples of minute volumes to be processed at physiological pH for structure and mass analysis, and allows the preparation characteristics to be finely tuned.

DOI: https://doi.org/10.1016/j.jsb.2011.11.001

# Connecting µ-fluidics to electron microscopy

Simon Kemmerling[1], Jörg Ziegler[1], Gabriel Schweighauser[1], Stefan A. Arnold[1], Dominic Giss[1], Shirley A. Müller[1], Philippe Ringler[1], Kenneth N. Goldie[1], Nils Goedecke[2], Andreas Hierlemann[2], Henning Stahlberg[1], Andreas Engel[1,3], and Thomas Braun[1,*]

[1] Center for Cellular Imaging and Nano Analytics (C-CINA), Biozentrum, Universität Basel, Basel, Switzerland

[2] Bio Engineering Laboratory (BEL), Department of Biosystems Science and Engineering (D-BSSE), ETH Zürich, Basel, Switzerland

[3] Department of Pharmacology, Case Western Reserve University, Cleveland, USA

* Corresponding Author
E-mail address: thomas.braun@unibas.ch
Tel. +41 (0)79 733 72 69
Fax: +41 (0)61 387 39 86
Address: Mattenstrasse 26, CH-4058 Basel, Switzerland

**A versatile methodology for electron microscopy (EM) grid preparation enabling total content sample analysis is presented. A microfluidic-dialysis conditioning module to desalt or mix samples with negative stain solution is used, combined with a robotic writing table to micro-pattern the EM grids. The method allows heterogeneous samples of minute volumes to be processed at physiological pH for structure and mass analysis, and allows the preparation characteristics to be finely tuned.**

**Keywords:** Electron microscopy, microfluidics, single-molecule analysis, mass and shape, systems biology

---

Abbreviations: AF, apoferritin; $AM_{6.5}$, ammonium molybdate at pH 6.5; BHK, Baby Hamster Kidney; $ddH_2O$, double-distilled water; EM, electron microscopy; ET, electron tomography; MPL, mass -per-length; MS, mass spectrometry; $NanoV_{8.0}$, NanoVan® at pH 8.0; $NanoW_{6.8}$, NanoW® at pH 6.8; $PTA_{7.0}$, phosphotungstic acid at pH 7.0; SD, standard deviation; STEM, scanning transmission electron microscopy; TEM, transmission electron microscopy; TMV, tobacco mosaic virus; $UA_{4.5}$, uranyl acetate at pH 4.5; $UA_{7.0}$ uranyl acetate at pH 7.0.

## 1. Introduction

Systems Biology aims to quantify the molecular elements of a biological system, to determine their interactions and to integrate this information into network models (Aderem, 2005). The development of comprehensive models requires experimental information about the spatial and temporal arrangements of the network components as well as their structure, a challenge that required a multi-resolution approach and the combination of different techniques (Aloy and Russell, 2006; Kherlopian et al., 2008). Cryo-electron tomography (cryo-ET) is the ultimate technique to reveal the spatial organisation of protein structures and macromolecular complexes in single cells (Ben-Harush et al., 2010; Lučić et al., 2005). Currently cryo-ET is restrained by several limitations, such as the size of the cell that can be analysed (maximum diameter of ~2 μm) (Leis et al., 2009), and by problems in data segmentation and in the template matching required for protein recognition (restricted to relatively large protein complexes) (Bohm et al., 2000). Indeed, many target structures can only be recognised if labelled with electron-dense markers (e.g., gold labels) (Nickell et al., 2006), which, despite recent progress (Kireev et al., 2008), often involves harsh preparative treatment of the cells. Furthermore, while ET delivers structural and spatial information, correlation of these with other methods such as mass spectroscopy (MS) (Aebersold and Mann, 2003) is difficult. A complementary approach is to physically lyse the cells and to subsequently write the entire sample onto electron microscopy (EM) grids for structure analysis by transmission EM (TEM), or mass analysis by scanning TEM (STEM). Ultimately, the use of microfluidic techniques offers the potential to analyse a single cell by making it possible to investigate protein ultrastructures and membrane fragments in lysates (Engel, 2010).

Here we present a lossless sample deposition method for EM (**Fig. 1**), which allows the handling of minute sample volumes and immobilization of the total sample content on EM grids to obtain, for example, the full cell inventory. This methodology is combined with a microfluidic sample-conditioning module. The constellation provides a new staining technique for heavy metal salts (negative stain) for TEM as well as specific desalting for mass measurements by STEM.

## 2. Materials and Methods

### *2.1. Stain Preparation*

The reservoir of the sample-conditioning module (**Fig. 2a**) was filled with different commonly used negative stains prepared in the following way: *Phosphothungstic acid ($PTA_{7.0}$)*: Sodium-phosphotungstate tribasic hydrate (Riedel-de Haen, Switzerland) was dissolved in double-distilled water ($ddH_2O$) to give a 1% or 2% (w/v) final concentration. The pH of the aqueous solution was adjusted to 7.0 using 1M potassium hydroxide; *Ammonium molybdate ($AM_{6.5}$)*: Ammonium molybdate (Aldrich, Switzerland) was dissolved in $ddH_2O$ to give a aqueous solution with a final concentration of 0.5% (w/v) at pH 6.5; *NanoVan® ($NV_{8.0}$)*: The 2% ready to use methylamine vanadate (Nanoprobes, USA) solution at pH 8.0 was diluted with $ddH_20$ to give a final concentration of 1% (w/v*); NanoW® ($NW_{6.8}$)*: The 2% ready to use methylamine tungstate

(Nanoprobes, USA) solution at pH 6.8 was diluted with $ddH_2O$ to give a final concentration of 1% (w/v); *Uranyl acetate ($UA_{4.5}$)*: Uranyl acetate was dissolved in $ddH_20$ to give a final concentration of 0.25% (w/v) at pH 4.5; *Buffered uranyl acetate ($UA_{7.0}$)*: To prepare UA at pH 7, the above 0.25% (w/v) uranyl acetate solution was mixed with an equal volume of a 20 mM oxalic acid solution. The pH was adjusted using 3% ammonium hydroxide, added slowly while stirring (Hayat, 2000). This resulted in a 0.12 % UA solution at pH 7.0.

### *2.2. Test samples*

Several samples were used for the initial tests and as a proof of concept: The chosen test samples apoferritin (AF; from equine spleen; Sigma, Switzerland) and tobacco mosaic virus (TMV; kindly supplied by Ruben Diaz-Avalos, New York Structural Biology Center, USA) are well characterized, and TMV is used as a standard for mass calibration in scanning transmission electron microscopy (STEM). The used test-samples were composed as follows: (1) A mixture of 0.05 mg/ml AF and 0.1 mg/ml TMV in phosphate buffered saline pH 7.4 (PBS; P4417, Sigma-Aldrich, Switzerland). (2) 0.05 mg/ml AF in PBS. (3) 0.1 mg/ml TMV in quartz-$ddH_2O$. (4) Baby Hamster Kidney (BHK) cell lysate in PBS (see next section).

### *2.3. BHK cell culture and lysis*

Attached Baby Hamster Kidney (BHK21; ECACC 85011433) cells were grown for 48h in a polystyrene T75-flask containing 30 ml of DHI-5 medium (see end of section) at 37° C, 100% air humidity, and 5% $CO_2$. To harvest the cells the medium was removed and the flask was washed with 7 ml of PBS. To detach the cells from the flask surface, 3 ml of trypsin-EDTA were added and the cells were incubated for 5 min at 37° C. Afterwards, 7 ml of DHI-5 medium were added and the detached cells were mixed using a pipet. 0.5 ml of the cell suspension was left in the flask and again incubated with 30 ml of fresh media for 48 h to obtain the next batch. The rest of the cell suspension was centrifuged twice and washed with PBS (48xg, 2min). The pellet was dissolved in 2ml of PBS. In an Eppendorf tube 200 µl of this cell suspension were further diluted with 800 µl of PBS and the cells were lysed by sonification for 2 min at 25 kHz while cooling.
DHI-5 medium is a mixture of DME (Dulbecco`s Modified Eagels Medium; D6171, Sigma, Switzerland), HamF12 (Nutrient Mixture F-12Ham; N8641, Sigma, Switzerland), and IMDM (Iscove`s Modified Dulbecco`s Medium, I3390, Sigma, Switzerland) media (1:1:2), supplemented with 5% FCS (Fetal Bovine Serum, E7524, Sigma, Switzerland) and complemented with non essential amino acids (MEM Non essential amino acid solution, M7145, Sigma, Switzerland), L-glutamine (L-Glutamine Solution, G7513, Sigma, Switzerland) and Vitamins (RPMI1640 Vitamins Solution, R7256, Sigma, Switzerland).

### *2.4. Microfluidic setup*

Samples were specifically treated and then deposited on carbon films covering 200 and 400 mesh Ni-TEM grids or on the special grids used for mass measurement (see below). This was achieved using a custom-built modular microfluidic setup (**Fig. 2a**) consisting of a syringe pump, a 10-port 2-position

valve, a custom-built sample conditioning module, a custom-built hand-over module, with functionalized nozzle, xyz-stage and several HPLC consumables (fused silica capillaries, PTFE tubing and connectors; BGB-analytic, Switzerland). The whole system is driven by the syringe pump (KDS210; Ismatec SA, Switzerland) and the sample is injected via a sample loop on the valve (Valco 10-port 2-position valve; BGB-analytic, Switzerland). All electronic components of the apparatus are controlled by a LabView-based custom-made software system (**supp. Fig. 1**), which features a macro language for flexible automation by coordination of the different modules. On request we will provide the software and the construction plans.

*2.5. Sample-conditioning module*

The sample-conditioning module consists of a custom-build reservoir that holds about 5 ml of solution (dialysis reservoir); either stain solution (for negative stain TEM) or 100 mM ammonium acetate prepared using quartz-dd$H_20$ (desalting). About 10-12 cm of a 13 kDa cut off cellulose fiber (Spectra/Pro® microdialysis fibers ID=200 µm; Spectrum Laboratories, USA) that holds 3-4 µl of sample at one time spans this reservoir. When the sample is pumped through this conditioning module at a rate of 2 µl/min, the dialysis time is about 2 min.

*2.6. Hand-over module and grid preparation*

The hand-over module deposits sub-microlitre sample volumes on EM grids by contact writing and can be programmed to automatically prepare a series of grids. The Ni-TEM grids are held in place by magnets and their carbon films are activated with atmospheric pressure helium cold-plasma (piezobrush® PZ1, Polyscience AG Switzerland) immediately before sample application. Initial tests showed that a 4 sec treatment at a distance of 1 cm from the plasma source gives comparable results to the conventional glow discharge (Aebi and Pollard, 1987), without destruction of the carbon film. A fully controllable micro-mechanical device (Physik Instrumente xyz micro-precision translation stages; Dyneos AG, Switzerland) brings a thin nozzle that is connected by micro-capillaries to the sample-conditioning module, in close proximity to the EM grid (**Fig. 2b**). After liquid contact, the grids are moved under the nozzle with sub-micrometer precision to create a micro-pattern of the sample on carbon in the form of a thin wet film. In this way 0.1-0.3 µl of stained or specifically desalted sample are 'written' on the grid, which is then air-dried. The degree of wetting obtained can be tuned by modifying the plasma treatment, and the writing can be optimized for the sample by adjusting the writing parameters. A defined combination of grid hydrophobicity (defined by plasma treatment parameters), writing speed, and surface tension of the applied solution (can be changed by the addition of ethanol traces), allowed a continuous line about 13 mm long and about 200 to 300 µm wide to be written (**Fig. 2c**).

*2.7. Nozzle preparation*

Commercially available fused silica capillaries (Polymicro) were used to make the nozzles. These were processed in the following way to optimize the liquid handling and direct the fluid onto the EM grids. The first 0.5-1.0 cm of the

polyimide coating of the fused silica capillaries was stripped away using hot chromosulfuric acid (Matthewson et al., 1997). Afterwards, the nozzle was extensively rinsed with $ddH_20$ to remove all traces of the acid. The fused silica was then cleaned by successively dipping the capillaries into $ddH_20$, ethanol and acetone for 10 min while shaking. Subsequently, the fused silica surface was activated by a 1 min treatment with cold atmospheric pressure helium plasma (piezobrush® PZ1, Polyscience AG, Switzerland). Immediately after plasma treatment the capillary tips were dipped into a silanization solution (~5% dimethyldichlorosilane in heptane; Silanization Solution 1, 85126, Fluka, Switzerland) for 1 hour and baked at 90° C for 4 hours. The stripped and silanized capillaries have an internal nozzle diameter of 50 μm.

### *2.8. Scanning Transmission Electron Microscopy*

A Vacuum Generators (East Grinstead, U.K.) HB-5 STEM interfaced to a modular computer system (Tietz Video and Image Processing Systems) was used. All samples were prepared on thin carbon films spanning gold sputtered, carbon-coated, 200-mesh-per-inch, gold-plated copper grids (STEM microscopy grids) (Müller et al., 1992). The aim was to determine whether samples leaving the microfluidics setup were clean and suitable for mass evaluation. After extensive rinse cycles for maintenance of the set-up, the sample dialysis reservoir was filled with quartz-$ddH_2O$. A stock solution of TMV in quartz-$ddH_2O$ was then passed through the conditioning module (micro-dialysis time of 2 min) and written to STEM microscopy grids by the hand-over module. The control grid, which also served as mass standard, was manually prepared in the conventional manner, i.e., a 5μl droplet of the same TMV stock was adsorbed to a STEM grid, blotted and washed on 8 droplets of 100mM ammonium bicarbonate solution prepared with quartz-$ddH_2O$, blotting after each step. All grids were allowed to air-dry. Series of digital 512 X 512 pixel, dark-field images were recorded from the grids at an acceleration voltage of 80 kV and a nominal magnification of 200,000x. The recording dose used varied between 290 and 635 electrons/$nm^2$. The images were evaluated with the MASDET program package as described previously (Krzyžánek et al., 2009). All mass-per-length (MPL) data were corrected for beam-induced mass-loss. The results from the control grid (mass standard) gave the instrumental scale factor, which was correspondingly applied to all measurements. The MPL data from the test grid were binned into a histogram and described by a Gaussian curve. The average MPL and standard deviation (SD) were also calculated and compared to the expected value of 133 kDa/$nm^2$ (Müller et al., 1992), and to the SD of the control grid results, respectively.

## 3. Results

The apparatus enables micro-patterning of EM grids with stained or desalted samples. It consists of two main units, (a) a sample-conditioning module for staining or desalting (or an inline combination of both), and (b) a hand-over module for micro-patterning the sample onto the grids (**Fig. 2a**). The instrument is designed for a prospective degree of automation and controlled by custom-written software (**supp. Fig. 1**). In the first step the sample is conditioned using

the micro-dialysis principle. This method was chosen because it is easy to integrate and because of its multiple application potential. In this sample-conditioning module, the sample flows through a cellulose fibre capillary (13 kDa cut-off) that extends through a reservoir of either negative stain solution or a volatile buffer (e.g., ammonium acetate or ammonium bicarbonate) in quartz double-distilled water ($ddH_2O$). Dialysis occurs as the sample liquid flows through the chamber, to either add the negative stain solution or remove undesired salts. The sample flow rate defines the dialysis time and can be adapted in a range from sec to min. Liquid contact writing is then used to deposit the sample on EM grids supporting a thin carbon film that was rendered partially hydrophilic by activation with an atmospheric pressure helium cold-plasma. This treatment replaced the conventional glow discharge technique (Aebi and Pollard, 1987). The piezo-driven plasma generation was chosen, as it is easier to integrate in an automated setup. The hand over unit is a micro-mechanical positioning device that brings a thin nozzle in close proximity to the grid. After liquid contact has been established, the grid is moved under the nozzle at sub-micrometer precision to create a meander-type micro-pattern of the sample on its carbon film (**Fig. 2b and 2c**). When this is finished, the nozzle is quickly moved up and down as the next grid is positioned (the time required is operator defined; minimum 0.5 sec). At present, a series of 26 grids can be written in sequence.

We have tested this new grid preparation method with a range of commonly used negative stains (Bremer et al., 1992), namely phosphotungstic acid at pH 7.0 ($PTA_{7.0}$), ammonium molybdate at pH 6.5 ($AM_{6.5}$), NanoVan at pH 8.0 ($NanoV_{8.0}$), NanoW at pH 6.8 ($NanoW_{6.8}$), and uranyl acetate at pH 4.5 ($UA_{4.5}$) and pH 7.0 ($UA_{7.0}$), and compared the results with grids prepared by conventional negative staining/blotting methods. Due to the effective staining behaviour of this method only half or even less (2 min micro-dialysis against 0.5% -1%) of the stain solution concentrations normally applied were used. A mixture of tobacco mosaic virus (TMV) and apoferritin (AF) in phosphate buffer system (PBS; 10 mM phosphate buffer, 2.7 mM KCl, 137 mM NaCl, pH 7.4) was employed to investigate the staining quality (**Fig. 3** left column, and **supp. Fig. 2**), while complete cell lysates of baby hamster kidney (BHK) cells allowed the staining behaviour for heterogeneous samples to be assessed (**Fig. 3** right column, and **supp. Fig. 3**). UA, one of the most commonly used negative stains employed in conventional negative stain EM, caused sample aggregation in our new method at both, pH 4.5 and pH 7.0 (**supp. Fig. 4**) and was not investigated further. Uranyl formate was not considered for testing, as a similar fixative effect as for UA has been reported (Bremer et al., 1992). The other stains examined gave excellent results for both test samples. When used at significantly lower concentrations than in classical staining methods, these stains provided good contrast in the EM and clearly revealed structural details. With the exception of $UA_{4.5}$, all of the stains were stabilized at physiological or close to physiological pH. When BHK cell lysates were examined in an analogous procedure, ultrastructural details, such as membrane fragments packed with proteins, filaments and individual proteins were all clearly resolved in the TEM with no sign of aggregation (**supp. Fig. 5**).

A STEM mass measurement achieves an accuracy of ± 5 – 10% depending on the sample and, working from an image, directly links the mass data to shape information (Engel, 2010). Initial tests made with TMV clearly showed that the modular microfluidic setup is capable of preparing the stringently clean grids required for these measurements (**Fig. 4a**). The carbon film of the written, air-dried grids of TMV in quartz-dd$H_2O$ dialysed against quartz-dd$H_2O$ was clean. Further, the mass-per-length measured for TMV was within 1.5% of that measured for the control grids, which were manually prepared in the conventional way and imaged in the same data acquisition session (**Fig. 4b**). Mass measurements require the removal of all non-volatile buffer components (Müller et al., 1992). The classic way to do this specific desalting is to wash the grid several times with quartz-dd$H_2O$ or a volatile buffer, e.g., ammonium acetate or bicarbonate, directly after sample adsorption. With the new grid preparation method, the required desalting is achieved before adsorption by dialysis. To avoid drastic pH changes and sample aggregation (**supp. Fig. 6**), micro-dialysis can be done against a volatile buffer, which allows the pH to be kept as close as possible to physiological values at all stages. Changes in the lateral aggregation of TMV after dialysis against ammonium bicarbonate illustrate the effect, and document the efficiency of the sample–conditioning module (**supp. Fig. 6**).

## 4. Discussion

Negative stain TEM is a standard method used in most electron microscopy laboratories involved in biology or biomedicine. In classical negative staining techniques for EM, a drop of sample (3 – 7 µl) is applied to the EM grid, which is then washed and stained. Each step is followed by a blotting procedure to remove excess liquid (**Fig. 1a**). Consequently, only a fraction of the sample and the stain remains on the grid. The amount of sample remaining depends on the adsorption, washing and blotting times, is often not reproducible, and the relative particle densities on the grid may be distorted by preferential adsorption of specific sample sub-fractions. Instead, our newly developed method adds the stain via dialysis prior to immobilization on the EM grid. Only 0.1-0.3 µl of the stain-mixed sample are required and no washing or blotting steps are involved (**Fig. 1b**). This allows a much higher proportion (close to 100%) of the initial sample to be deposited on the EM grid, so that the true relative ratios between the different sample constituents are maintained (**supp. Fig. 7**). Moreover the stain density is controlled by the heavy metal concentration in the reservoir and the flow rate and can be easily tuned (**Fig. 5**).

In our hands, the automated procedure is more reproducible than manual staining, especially for „difficult" stains such as AM, nanoW and PTA. This new method without any blotting or washing steps provides good contrast even for stains with weak electron scattering properties; the contrast is significantly higher than that achieved manually. Furthermore, the stain seems to be homogenously distributed around the particles, a fact that might be important for subsequent data analysis steps, such as alignments. Both, the contrast and the stain distribution attained with low scattering stains, may be favourably influenced by the preincubation of the protein complexes before adsorption to the grid surface as the stain has more time to penetrate the fine structures of the

proteins. However, the resolution still appears to be limited by the grain size of the stain. Visually, AM seems to exhibit an excellent balance between stain grain size, contrast and "dynamic range" (**supp. Fig. 5c**). Moreover, their tolerance to phosphate buffers, the most frequently used buffers in biochemistry and cell biology, and the possibility to adapt their pH makes AM and PTA applicable to a broad spectrum of samples.
In the future, the hand-over module will be developed to allow grid preparation for higher resolution techniques such as cryo-EM where the ice thickness is a critical, contrast-determining property. To this end, the grid temperature will be kept at the thaw point to avoid evaporation or condensation of the liquid during writing. Subsequently, the grid will be shot into liquid ethane. Alternatively, it will be freeze-dried to allow improved mass and shape measurements by STEM.

The microfluidic sample preparation platform presented here has the potential to become an important tool not only for systems biology but also for EM in general, which demands reproducible, quantitative sample grid preparation and assessment. The possibility of micro-patterning EM grids will allow a more systematic and convenient analysis of complex samples in the future. Combined with microfluidic methods for cell lysis, protein separation and labelling, this method for total cell content analysis for structure and mass offers the potential to optimally complement other experimental system biology techniques such as MS (Picotti et al., 2009) and ET (Barcena and Koster, 2009; Förster et al., 2010). For this particular application, the raw images must be analyzed by feature matching methods (Bohm et al., 2000; Förster et al., 2010; Penczek and Huang, 2004) to obtain quantitative information. To aid the analysis, a visual library will be constructed containing the projections of *a priori* target molecules. The raw data images recorded from samples prepared in a lossless manner will be segmented by a hierarchical algorithm (Adiga et al., 2005; Coudray et al., 2007), and the various particles present classified according to their size and shape. Shape matching will also allow the link to be made between negative stain and STEM images, combining the higher resolution and high contrast of the TEM projections with the mass obtained from unstained samples by STEM. Finally, cross-correlation techniques will be used to assign the TEM projections to the most probable match in the visual library (Förster et al., 2010).

The outlined automated sample preparation technique opens the way for a new visual proteomics approach. Ultimately it will allow the total content of a single cell or miniscule tissue region to be examined by EM. It will then become possible to assemble complete ultrastructural libraries from cells or tissues. The method will make the structural study of the various cellular components on the single molecule level possible. We foresee the method as a valuable tool to study complex biological systems, complementing other systems-biological methods.

## Acknowledgements

We thank Mohamed Chami, Christopher Bleck (C-CINA) and the mechanical work-shop of the Biozentrum of the University Basel for their discussions and aid. The project is supported by the SystemsX.ch initiative (CINA, granted to A.E.

and H.S.); the STEM microscopy by the Swiss National Science Foundation (Grant 3100A0-108299 to A.E. and the NCCR Nanoscience).

## Appendix A. Supplemental material

## References

Aderem, A., 2005. Systems biology: its practice and challenges. Cell 121, 511-513.

Adiga, U., Baxter, W.T., Hall, R.J., Rockel, B., Rath, B.K., Frank, J., Glaeser, R., 2005. Particle picking by segmentation: a comparative study with SPIDER-based manual particle picking. J. Struct. Biol. 152, 211-220.

Aebersold, R., Mann, M., 2003. Mass spectrometry-based proteomics. Nature 422, 198-207.

Aebi, U., Pollard, T.D., 1987. A glow discharge unit to render electron microscope grids and other surfaces hydrophilic. J. Elect. Microsc. Tech. 7, 29-33.

Aloy, P., Russell, R.B., 2006. Structural systems biology: modelling protein interactions. Nat. Rev. Molec. Cell Biol. 7, 188-197.

Barcena, M., Koster, A.J., 2009. Electron tomography in life science. Semin. Cell Dev. Biol. 20, 920-930.

Ben-Harush, K., Maimon, T., Patla, I., Villa, E., Medalia, O., 2010. Visualizing cellular processes at the molecular level by cryo-electron tomography. J. Cell Sci. 123, 7-12.

Bohm, J., Frangakis, A.S., Hegerl, R., Nickell, S., Typke, D., Baumeister, W., 2000. Toward detecting and identifying macromolecules in a cellular context: template matching applied to electron tomograms. Proc. Nat. Acad. Sci. USA 97, 14245-14250.

Bremer, A., Henn, C., Engel, A., Baumeister, W., Aebi, U., 1992. Has negative staining still a place in biomacromolecular electron microscopy? Ultramicroscopy 46, 85-111.

Coudray, N., Buessler, J.L., Kihl, H., Urban, J.P., 2007. Multi-scale and first derivative analysis for edge detection in TEM images. Image Analysis and Recognition, Proceedings 4633, 1005-1016.

Engel, A., 2010. Assessing Biological Samples with Scanning Probes. Single Molecule Spectroscopy in Chemistry, Physics and Biology 96, 417-431.

Förster, F., Han, B.G., Beck, M., 2010. Visual Proteomics. Methods in Enzymology, Vol 483: Cryo-EM, Part C: Analyses, Interpretation, and Case Studies 483, 215-243.

Hayat, M.A., 2000. Principles and Techniques of Electron Microscopy. Biological Applications. 4th ed. Cambridge University Press, Cambridge.

Kherlopian, A.R., Song, T., Duan, Q., Neimark, M.a., Po, M.J., Gohagan, et al., 2008. A review of imaging techniques for systems biology. BMC Syst. Biol. 2, 74-74.

Kireev, I., Lakonishok, M., Liu, W., Joshi, V.N., Powell, R., et al. , 2008. *In vivo* immunogold labeling confirms large-scale chromatin folding motifs. Nat. Methods 5, 311-313.

Krzyžánek, V., Müller, S.A., Engel, A., Reichelt, R., 2009. MASDET-A fast and user-friendly multiplatform software for mass determination by dark-field electron microscopy. J. Struct. Biol. 165, 78-87.

Leis, A., Rockel, B., Andrees, L., Baumeister, W., 2009. Visualizing cells at the nanoscale. Trends Biochem. Sci. 34, 60-70.

Lučić, V., Förster, F., Baumeister, W., 2005. Structural studies by electron tomography: from cells to molecules. Ann. Rev. Biochem. 74, 833-865.

Matthewson, M.J., Kurkjian, C.R., Hamblin, J.R., 1997. Acid stripping of fused silica optical fibers without strength degradation. J. Lightwave Technol. 15, 490-497.

Müller, S.A., Goldie, K., Burki, R., Haring, R., Engel, A., 1992. Factors influencing the precision of quantitative scanning transmission electron microscopy. Ultramicroscopy 46, 317-334.

Nickell, S., Kofler, C., Leis, A.P., Baumeister, W., 2006. Perspectives A visual approach to proteomics. Nature Rev. Molec. Cell Biol. 7, 225-230.

Penczek, P.A., Huang, Z., 2004. Application of template matching technique to particle detection in electron micrographs. J. Struct. Biol. 145, 29-40.

Picotti, P., Bodenmiller, B., Mueller, L.N., Domon, B., Aebersold, R., 2009. Full dynamic range proteome analysis of *S. cerevisiae* by targeted proteomics. Cell 138, 795-806.

## Figure captions

**Figure 1:** Schema of negative staining methods for EM. (a) Classical negative staining by hand: The sample is absorbed to the carbon film of an EM grid and the grid is blotted to remove the excess sample solution. The absorption time and the specific absorption properties of the sample components determine the fraction of the sample that is immobilized. A wash and blot cycle sometimes follows (not shown). The grid is then incubated with the negative stain solution of choice, followed by another blotting step to remove excess stain solution. The grid is left to air-dry before investigation in the electron microscope. This method only immobilizes a fraction of the sample on the grid. (b) The here developed microfluidic negative staining approach: A very small amount (0.1-0.3 µl) of stain-mixed sample is applied to the grid via a nozzle of 50 µm inner diameter. The grid is then air-dried without any blotting. With this method the entire sample is immobilized on the grid. Additionally, the micro-precision of the writing process allows a meander-type micro-pattern of stained sample to be created on the carbon film.

**Figure 2:** Sample-conditioning module and micro-patterning device. (a) Schematic representation of the main components and the meander-type writing pattern. (b) Nozzle positioned above an EM grid on the xyz-stage. Inset: enlarged view; the arrow indicates the nozzle tip. (c) TEM image of a micro-patterned grid showing a section of the six 200-300-µm-wide lines of a $PTA_{7.0}$ stained sample (diagonal dark grey lines) written on an EM grid (black) and the empty carbon film in between (light grey). Scale bar: 200 µm.

**Figure 3:** Gallery of TEM images. This selection shows TEM images of the two test samples prepared with the setup and different stains. (Left column) Mixture of AF and TMV. For all negative stains the central channel and the 23Å repeat of TMV and the sub-structure of the AF is visible. (Right column) BHK cell lysate showing typical membrane structures with integrated membrane proteins that exhibit the shape of ATPases. (Rows) Samples in PBS were conditioned with 1% $PTA_{7.0}$, 0.5% $AM_{6.5}$, 1% $NanoV_{8.0}$, and 1% (left) or 2% (right) $NanoW_{6.8}$. Scale bars: 100 nm; insets depict three-fold enlarged regions of the TMV. (for more images see Supplementary Figs. 2 and 3).

**Figure 4**: Mass measurement of TMV by STEM to test the preparation quality and cleanliness delivered by the microfluidic setup. (a) STEM dark-field image of unstained, air-dried TMV written on a STEM microscopy grid for mass measurement. TMV (0.1 mg/ml) in quartz-dd$H_2O$ was dialysed against quartz-dd$H_2O$ for 2 min in the sample-conditioning module and written onto the grid. The thin carbon film beneath the TMV rods is clean (uniform dark regions). A small segment of the gold-sputtered, perforated thick carbon layer supporting this film is also visible (bright irregular region upper right). (b) Mass-per-length histogram of correspondingly written TMV. After scaling according to the mass standard, the determined average mass-per-length, 135 ± 6 kDa/nm, is within 1.5% of the expected value, 133 kDa/nm (Müller et al., 1992). Further, the standard deviation of the data set is comparable to that of the mass standard, ± 4 kDa/nm, which was prepared in the conventional way (see Materials and Methods). Scale bar: 100 nm.

**Figure 5:** Fine-tuning of the stain density: Representative images of samples conditioned with different $PTA_{7.0}$ concentrations, clearly showing the different stain densities. The mixture of AF and TMV in PBS was conditioned with 0.5%, 1% or 1.5% of $PTA_{7.0}$. This demonstrates that easy and reproducible stain density fine-tuning is possible to adapt to different samples or to reveal different details of the same sample. Combined with several applicable stains with distinct properties, this offers the potential to individually optimize the staining for a certain sample or certain sample details. Scale bars: 100nm; insets depict three-fold enlarged regions of the TMV.

Figure 1

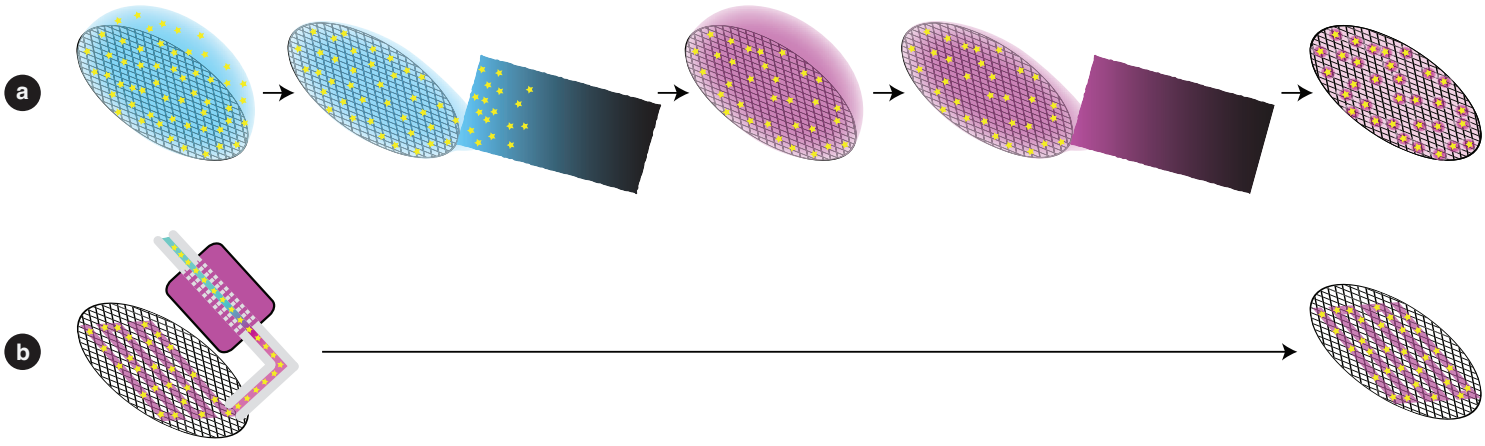

Figure 2

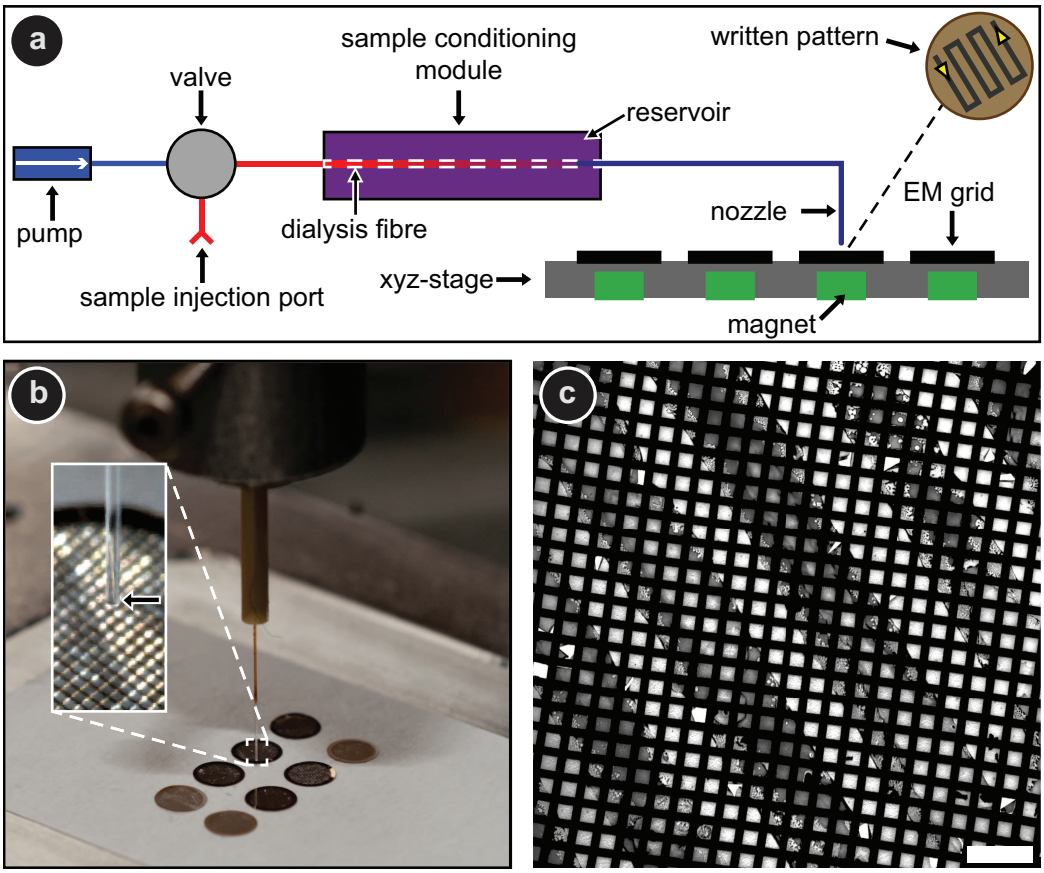
a
sample conditioning module
written pattern
valve
reservoir
pump
dialysis fibre
nozzle
EM grid
sample injection port
xyz-stage
magnet
b
c

Figure 3

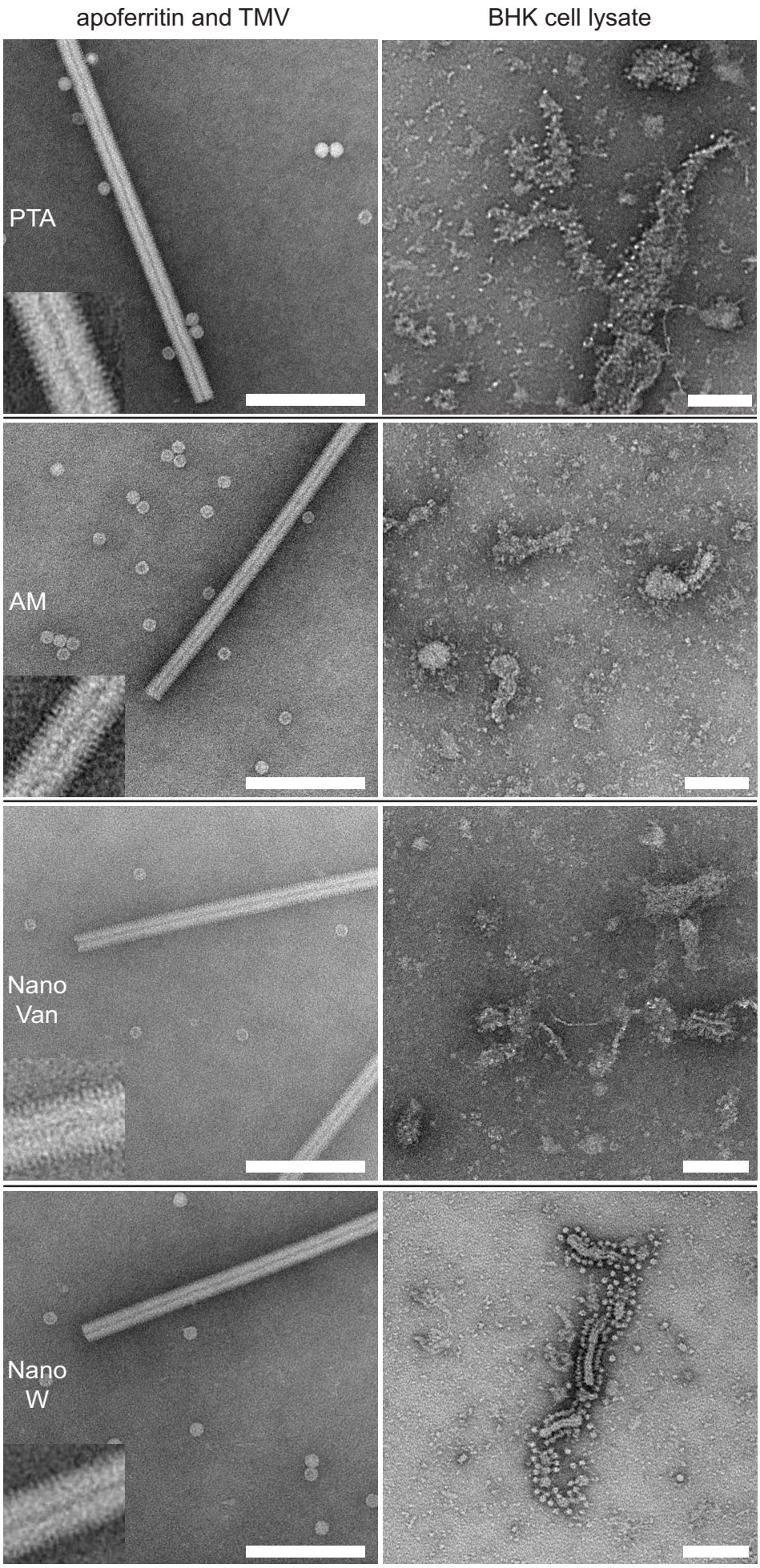

Figure 4

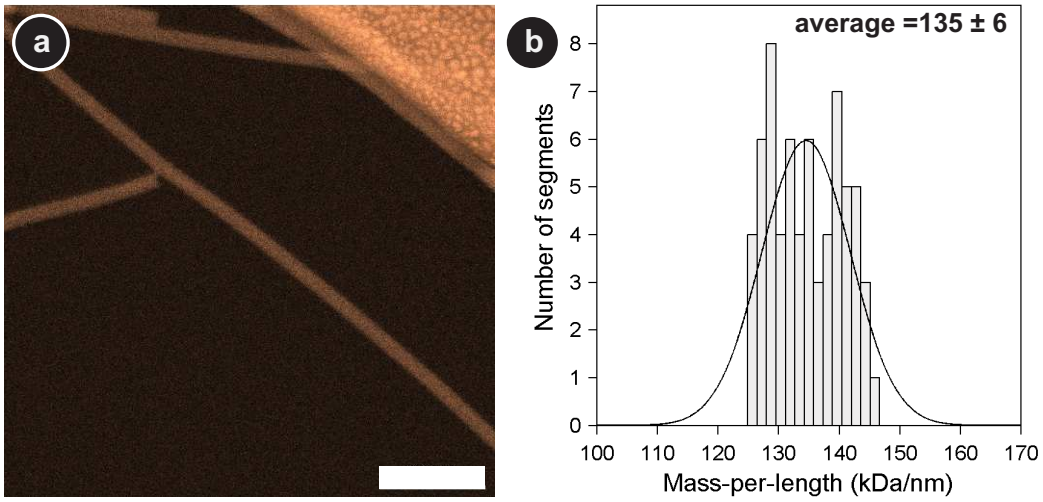
a
b
average =135 ± 6
Number of segments
0
1
2
3
4
5
6
7
8
100
110
120
130
140
150
160
170
Mass-per-length (kDa/nm)

Figure 5

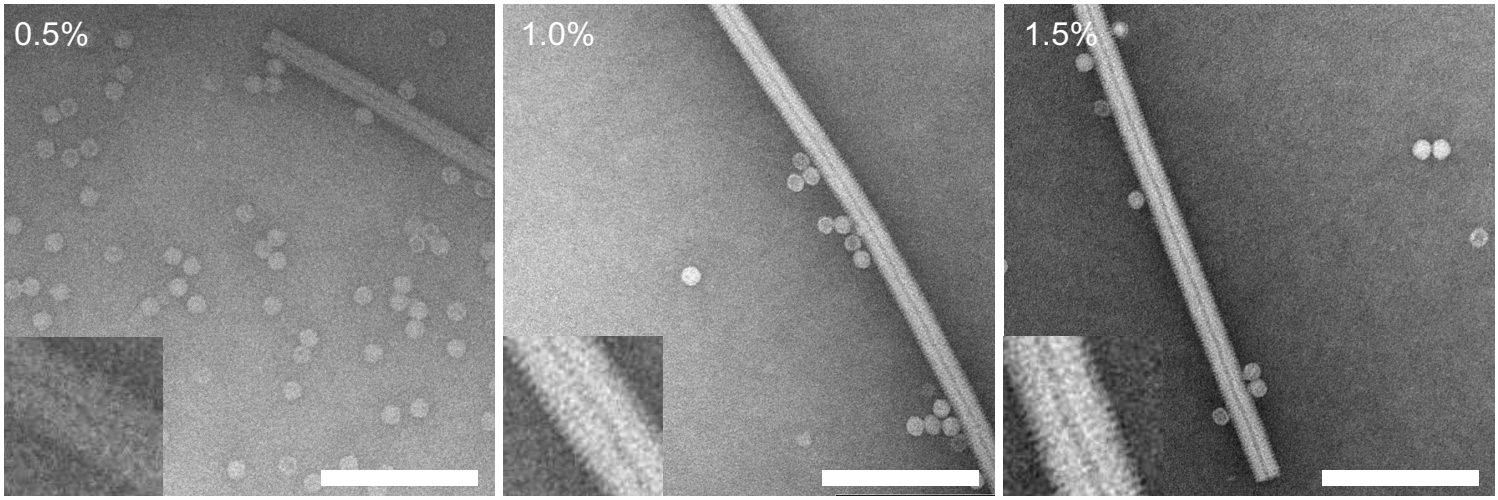

# Supplementary Material

# Connecting µ-fluidics to electron microscopy

Simon Kemmerling[1], Jörg Ziegler[1], Gabriel Schweighauser[1], Stefan A. Arnold[1], Dominic Giss[1], Shirley A. Müller[1], Philippe Ringler[1], Kenneth N. Goldie[1], Nils Goedecke[2], Andreas Hierlemann[2], Henning Stahlberg[1], Andreas Engel[1,3], and Thomas Braun[1]*

[1] Center for Cellular Imaging and Nano Analytics (C-CINA), Biozentrum, Universität Basel, Basel, Switzerland

[2] Bio Engineering Laboratory (BEL), Department of Biosystems Science and Engineering (D-BSSE), ETHZ, Basel

[3] Department of Pharmacology, Case Western Reserve University, Cleveland, USA

* Corresponding Author
E-mail address: thomas.braun@unibas.ch
Tel. +41 (0)79 733 72 69
Fax: +41 (0)61 387 39 86
Address: Mattenstrasse 26, CH-4058 Basel, Switzerland



| | |
|---|---|
| **Supplementary Figure 1** | Screenshot of the LabView-based control software |
| **Supplementary Figure 2** | Gallery of negatively stained test samples |
| **Supplementary Figure 3** | Gallery of negatively stained BHK lysate |
| **Supplementary Figure 4** | UA staining results |
| **Supplementary Figure 5** | Images of BHK cell lysate demonstrating the absence of aggregation. |
| **Supplementary Figure 6** | TMV preparation for STEM |
| **Supplementary Figure 7** | Comparison of manual and automated grid preparation |

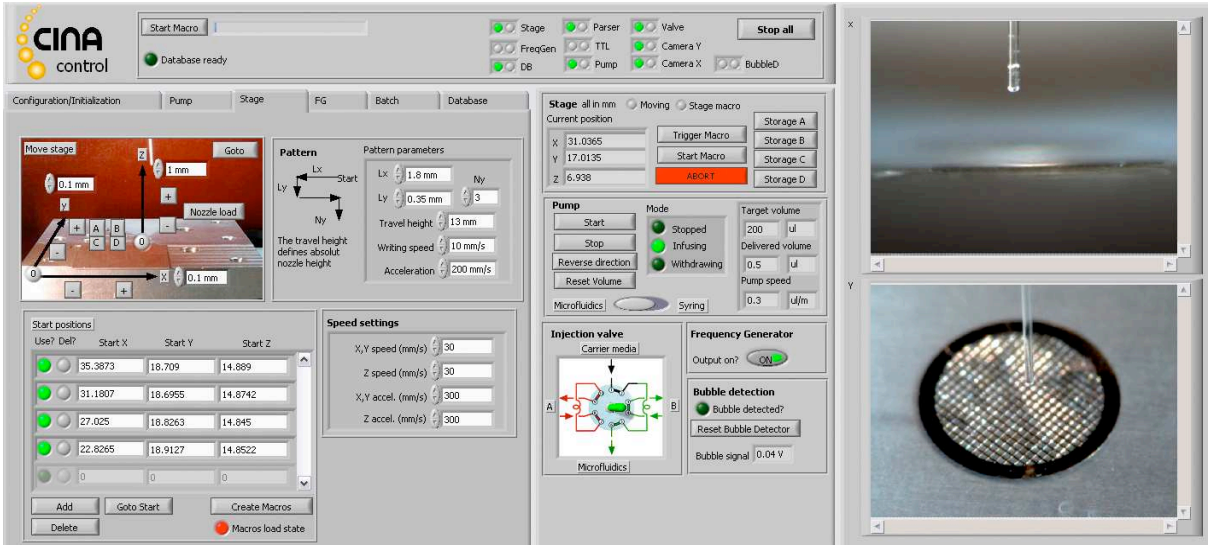


**Supplementary Figure 1:** Graphical user interface of the LabView-based control software: This self-written software allows all setup components to be controlled and examined. It shows the status of all components and two cameras installed at different angles deliver live images of the nozzle and the grid being processed, respectively. The parameters controlling the components can either be set individually or via a macro language that was integrated to facilitate automation.

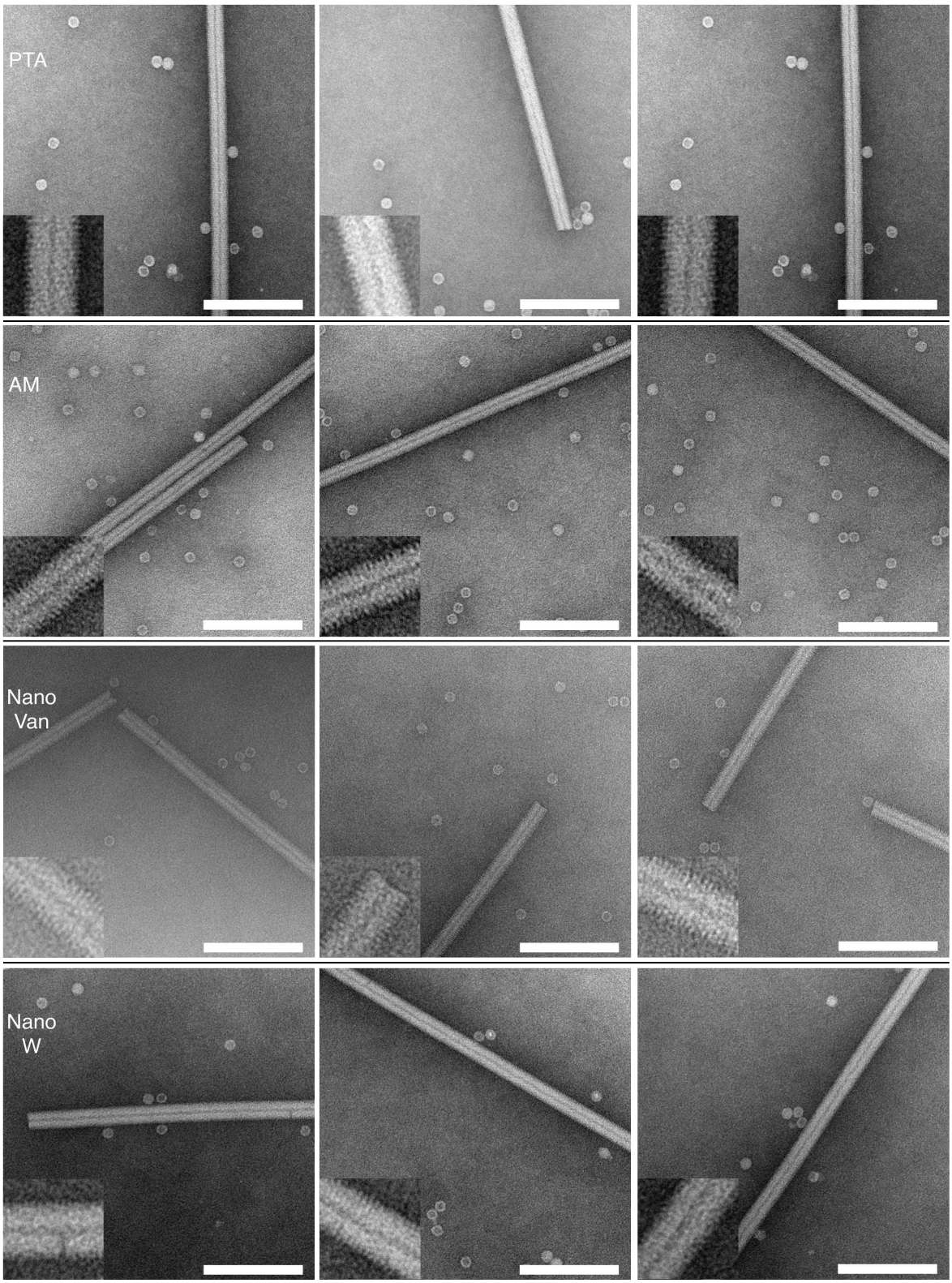


**Supplementary Figure 2**: Further examples of negatively stained TMV and AF samples. For all four stains the ultrastructure of TMV and AF is well preserved and the surrounding background shows a smooth fine grain. Samples were conditioned with 1% $PTA_{7.0}$, 0.5% $AM_{6.5}$, 1% $NanoV_{8.0}$, and 1% $NanoW_{6.8}$. Scale bars: 100 nm; the insets depict three-fold enlarged regions of the TMV.

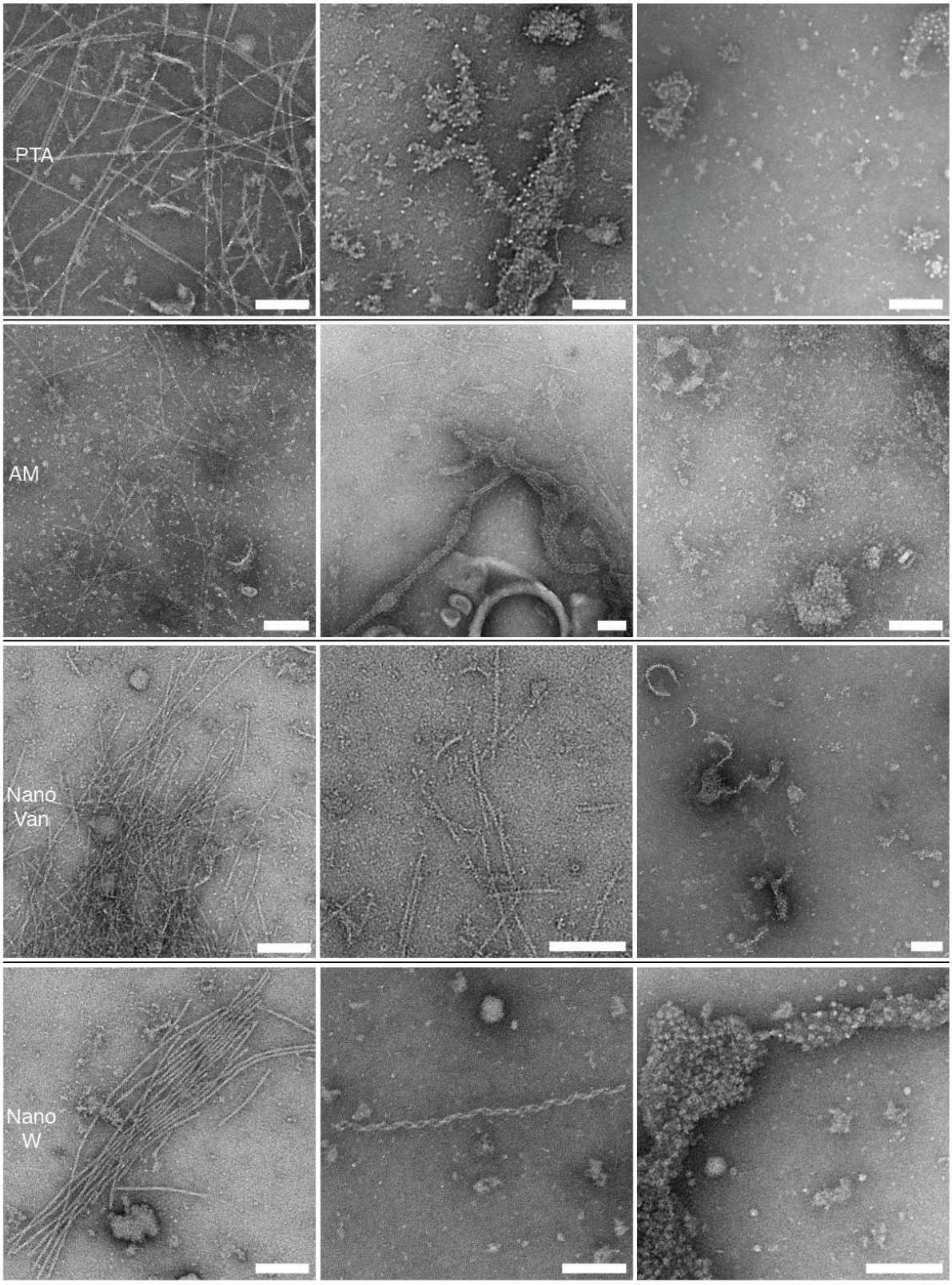


**Supplementary Figure 3:** Further examples of negatively stained BHK lysate for the four different stains, revealing structures resembling actin filaments (e.g. top left) and protein-packed membranes (e.g. top center). Samples were conditioned with 2% $PTA_{7.0}$, 0.5% $AM_{6.5}$, 1% $NanoV_{8.0}$, and 2% $NanoW_{6.8}$. Scale bars: 100 nm.

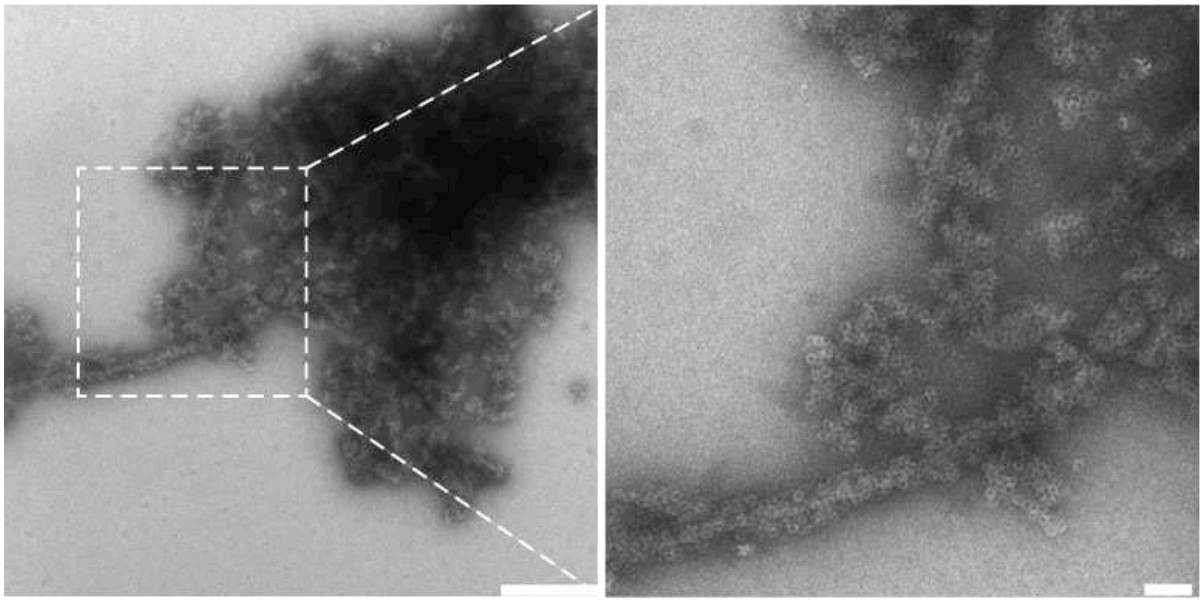

**Supplementary Figure 4**: UA staining results. A TEM image of aggregated TMV and AF conditioned with 0.25 % $UA_{4.5}$. An enlarged view of the marked region is shown on the right. Other experiments showed, that there is serious precipitation when $UA_{4.5}$ is mixed with the sample at concentrations above 0.5 % and dried down on the grid (data not shown), even if the buffer does not contain phosphate; the sample was in HEPES or $ddH_2O$. Decreasing the UA concentration to 0.25% or below prevented the formation of precipitates, but the fixation property of UA caused sample aggregation when stain and sample were mixed prior to immobilization on the grid. Furthermore, buffering the UA solution at a concentration of 0.25% or below at pH 7 could not prevent this sample aggregation. Scale bars: (left) 250 µm; (right) 50µm.

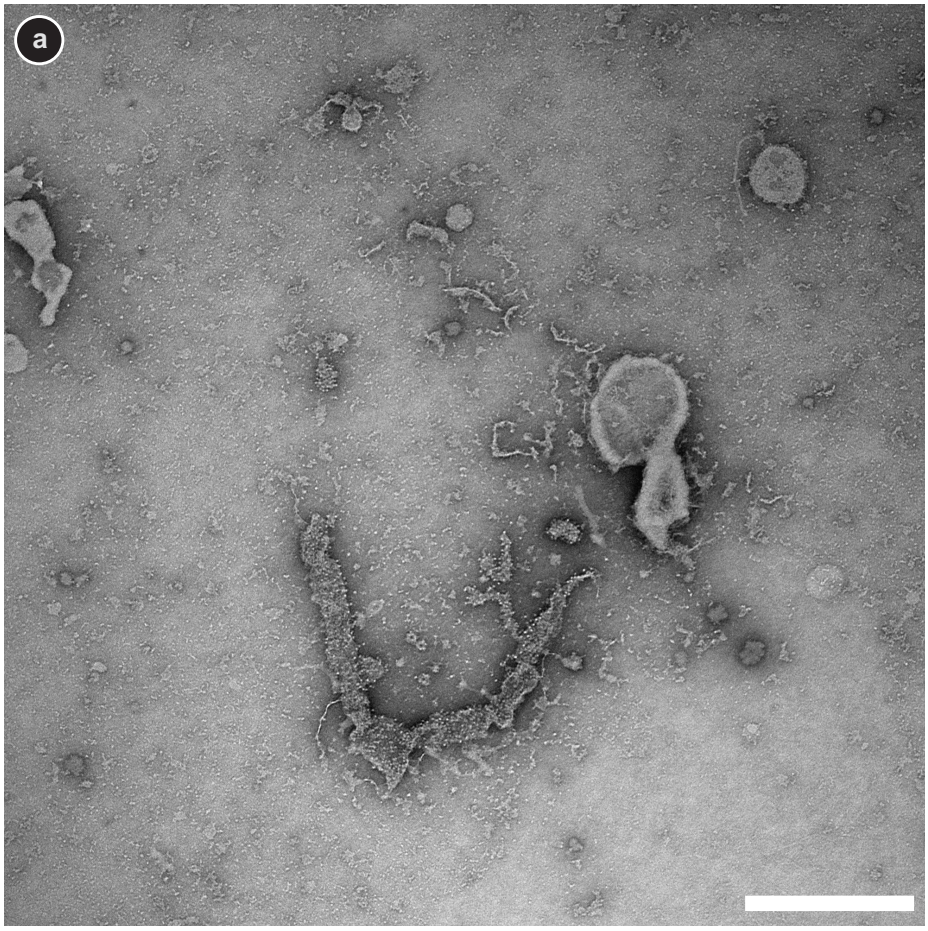
a

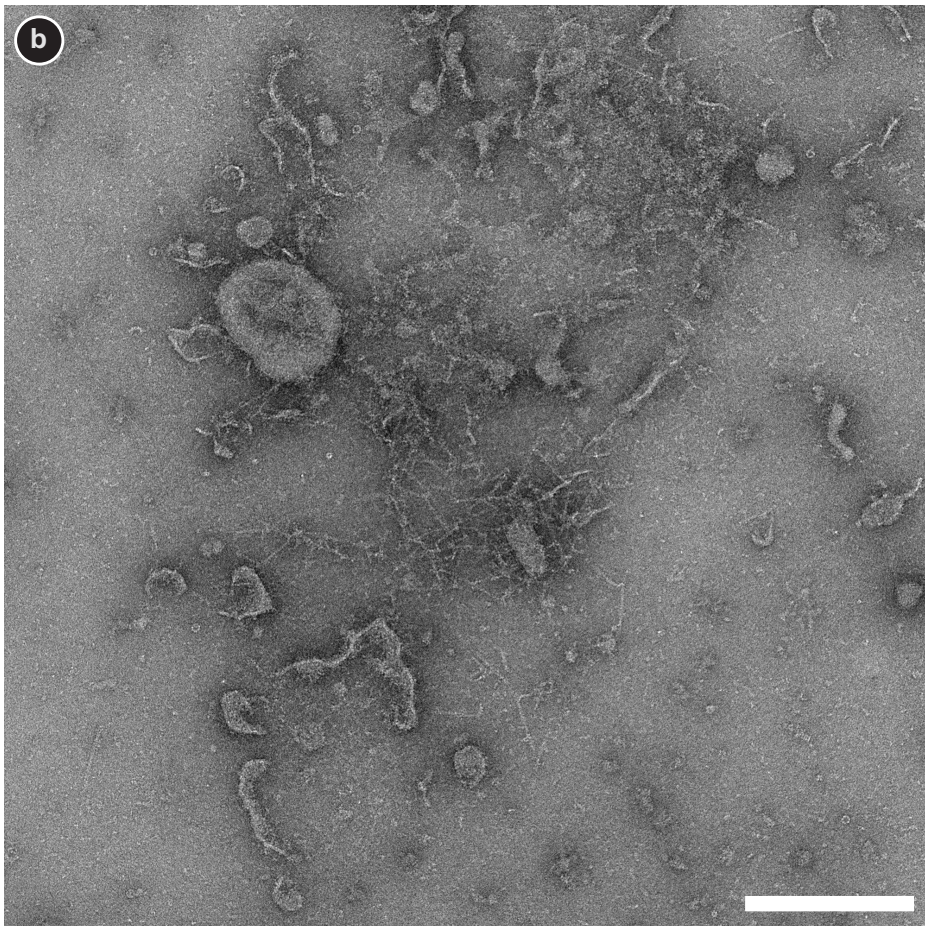
b

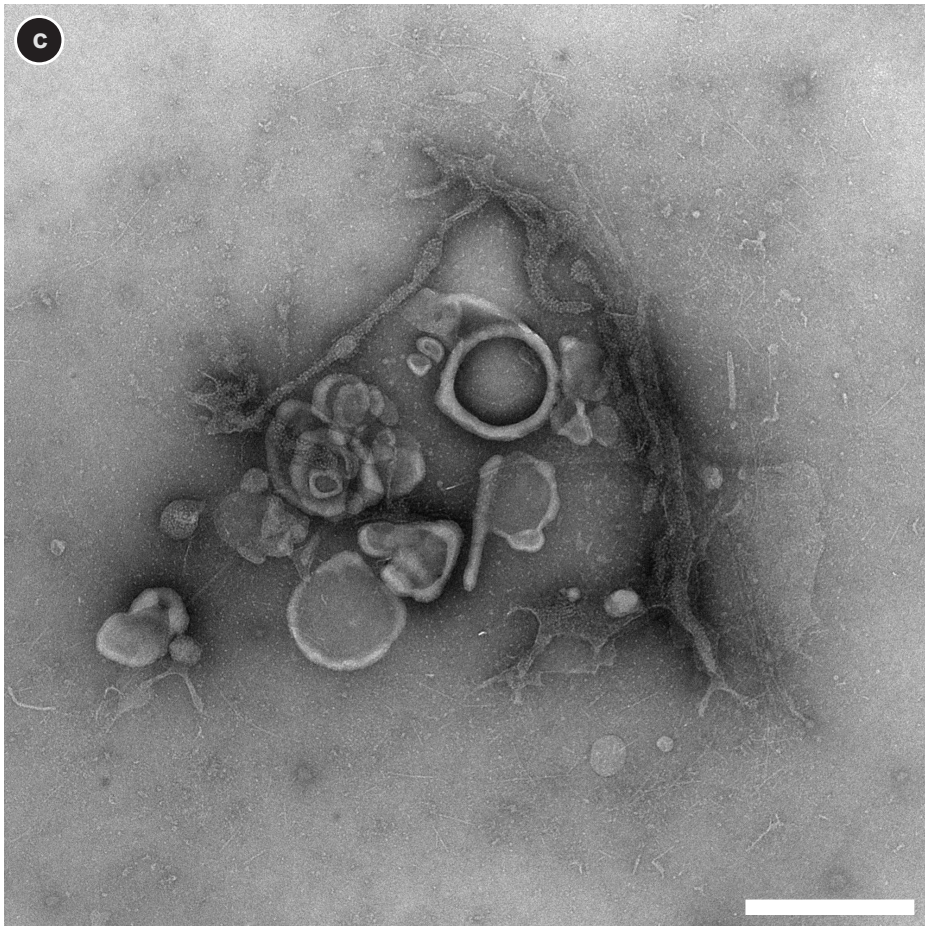
c

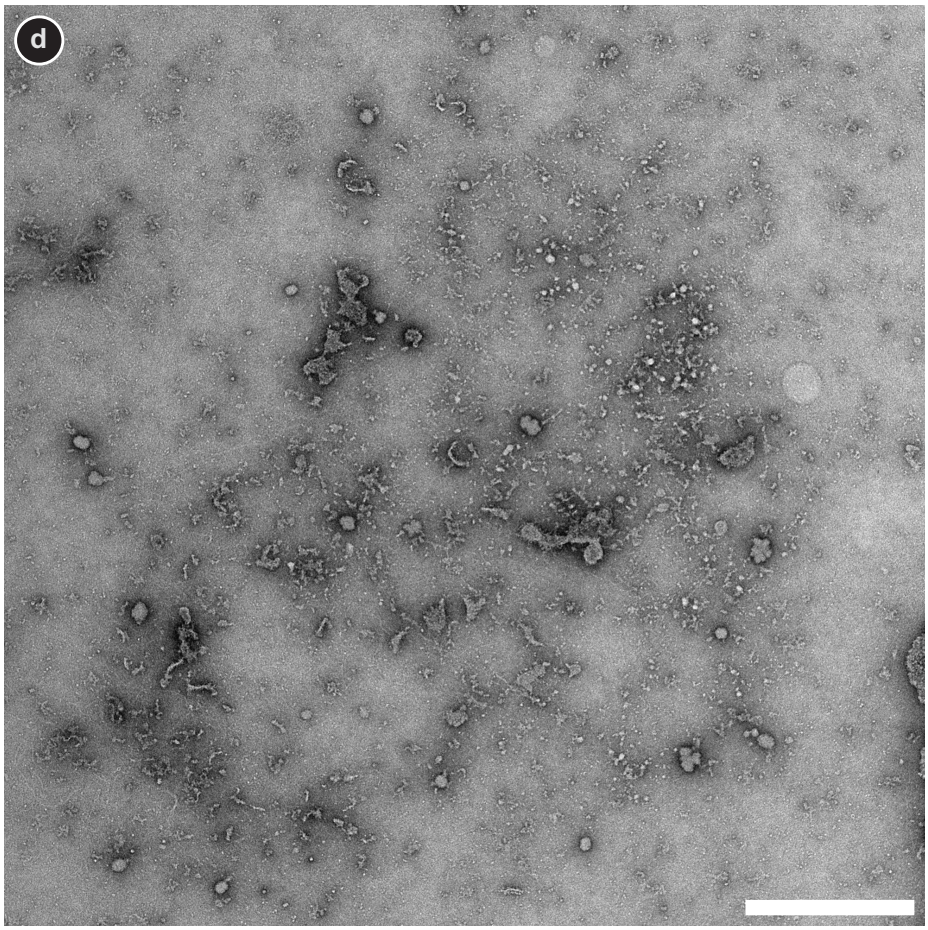
d

**Supplementary Figure 5**: Images of BHK cell lysate demonstrating the absence of aggregation. The overview images show soluble proteins, membrane patches and filaments; there is no sign of aggregation. The sample in PBS was conditioned with (a) 2% $PTA_{7.0}$. (b) 0.5% $AM_{6.5}$. (c)1% $NanoV_{8.0}$. (d) 2% $NanoW_{6.8}$. Scale bars: 500 nm.

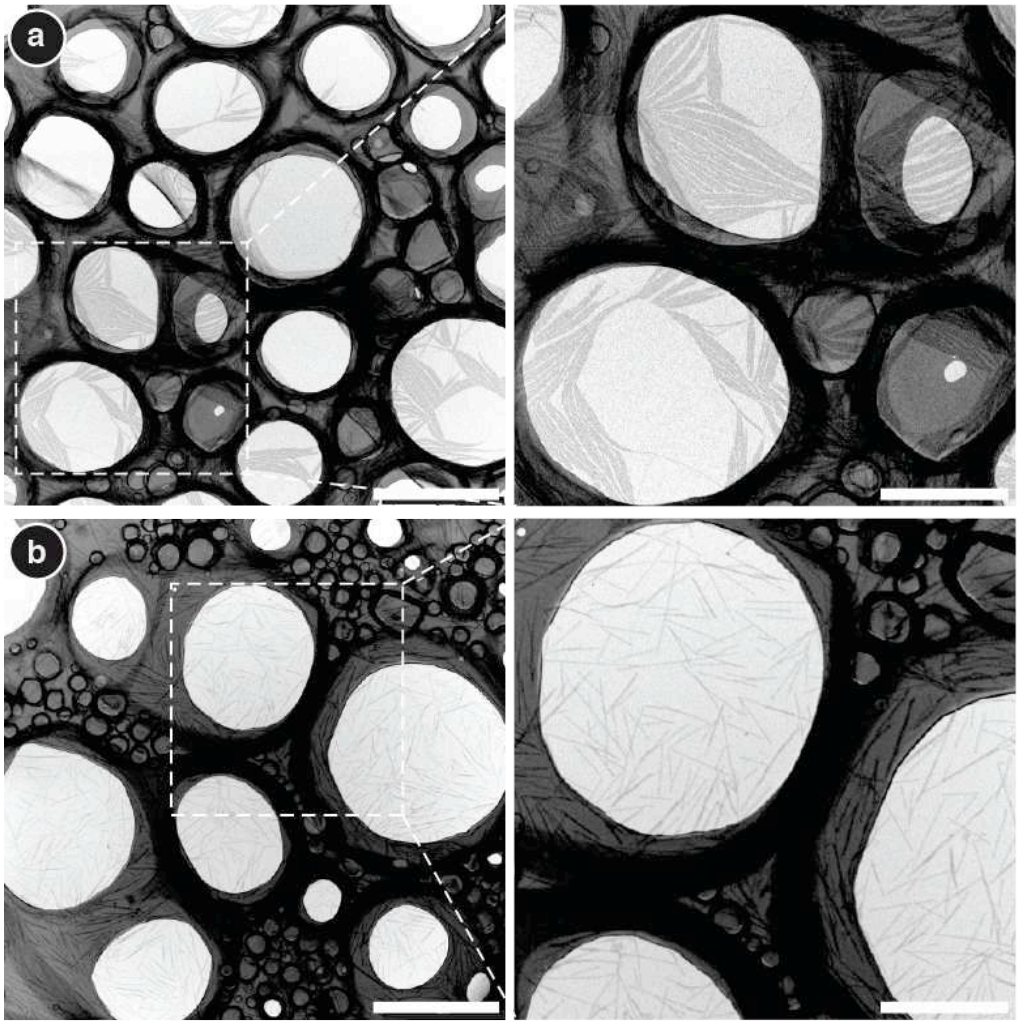


**Supplementary Figure 6**: TEM images of unstained TMV written on STEM grids after passage through the sample preparation module: (a) TMV in quartz-dd$H_20$, after micro-dialysis against quartz-dd$H_20$. The rods tend to aggregate, which would hinder mass determination; only a few are well separated from their neighbors. (b) TMV in quartz-dd$H_20$, after micro-dialysis against 100 mM ammonium bicarbonate buffer. The rods are homogeneously distributed over the grid and generally well separated. The marked change in aggregation shows that conditioning was effective. The results illustrate that even robust samples like TMV benefit from solutions that are buffered close to physiologic pH. Scale bars: (left column) 500 µm; (right column) 250 µm.

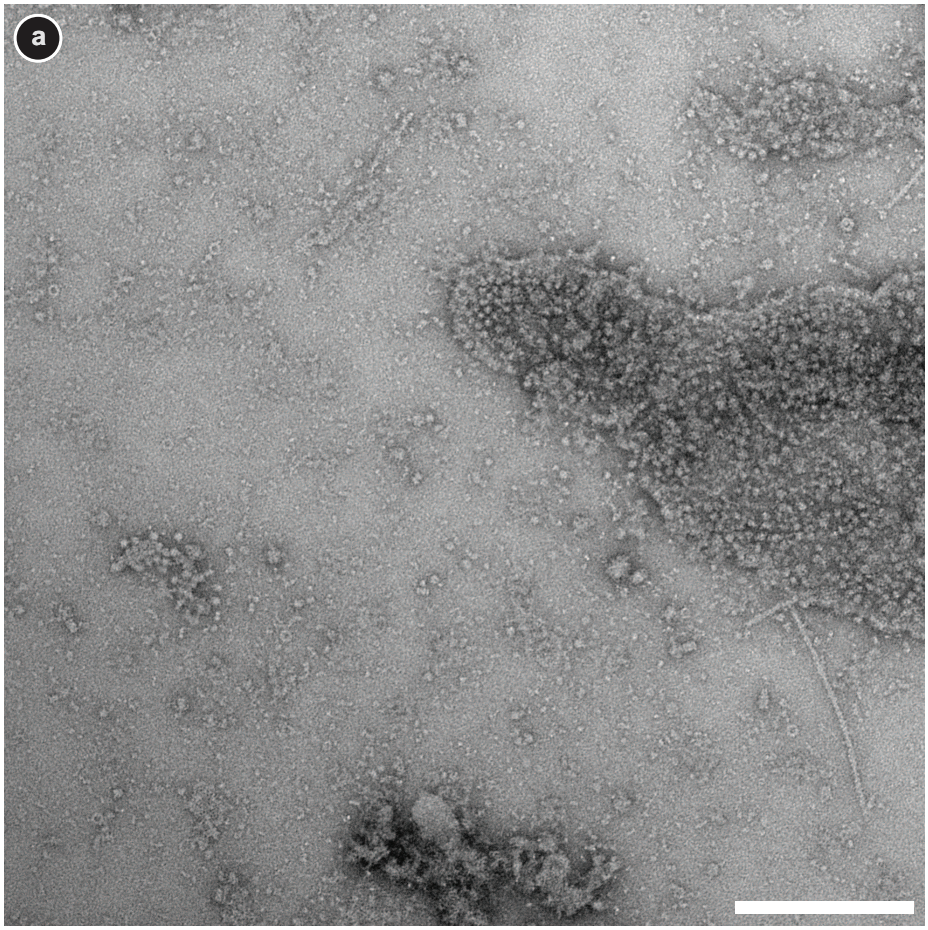
a

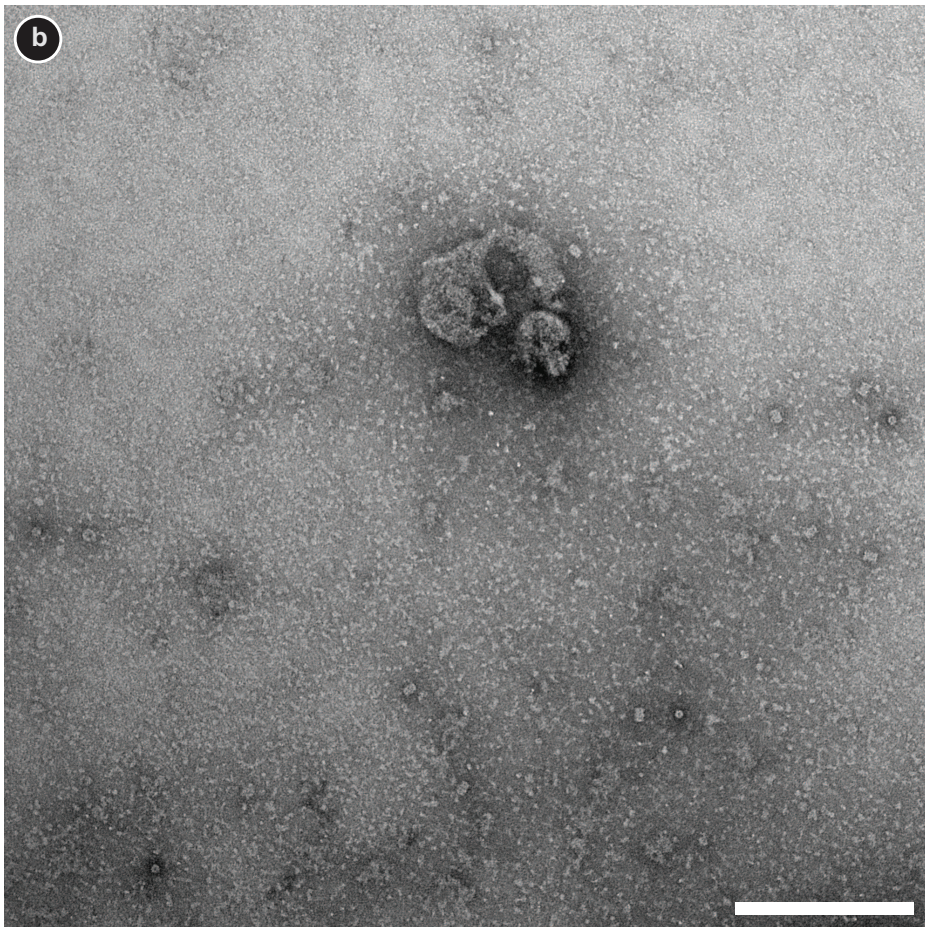
b

**Supplementary Figure 7:** Comparison of manual and automated grid preparation. Representative overview images of lysate from heat-shocked (46°C for 60min) BHK cells. (a) Prepared with the setup and conditioned with 1% $NanoW_{6.8}$. (b) Manually prepared (1 min sample adsorption followed by four wash steps of 5 sec) and stained with 2% $NanoW_{6.8}$ (two times 5 µl of stain for 10 sec). Besides the heat-shock proteins that can be observed with both preparation methods the setup preparation method reveals more sample constituents. Large "protein packed" membrane patches as well as filaments are abundant and clearly visible with structural details. These components were not observed when the grids were prepared by hand. Scale bars: 200 nm.